Journal of Digital Imaging

A Technique for Simulating the Effect of Dose Reduction on Image Quality in Digital Chest Radiography

Wouter J.H. Veldkamp, Lucia J.M. Kroft, Jan Pieter A. van Delft, and Jacob Geleijns

Purpose: **The purpose of this study is to provide a pragmatic tool for studying the relationship between dose and image quality in clinical chest images. To achieve this, we developed a technique for simulating the effect of dose reduction on image quality of digital chest images.** ***Materials and Methods:*** **The technique was developed for a digital charge-coupled-device (CCD) chest unit with slot-scan acquisition. Raw pixel values were scaled to a lower dose level, and a random number representing noise to each specific pixel value was added. After adding noise, raw images were post processed in the standard way. Validation was performed by comparing pixel standard deviation, as a measure of noise, in simulated images with images acquired at actual lower doses. To achieve this, a uniform test object and an anthropomorphic phantom were used. Additionally, noise power spectra of simulated and actual images were compared. Also, detectability of simulated lesions was investigated using a model observer.** ***Results:*** **The mean difference in noise values between simulated and real lower-dose phantom images was smaller than 5% for relevant clinical settings. Noise power spectra appeared to be comparable on average but simulated images showed slightly higher noise levels for higher spatial frequencies and slightly lower noise levels for lower spatial frequencies. Comparable detection performance was shown in simulated and actual images with slightly worse detectability for simulated lower dose images.** ***Conclusion:*** **We have developed and validated a method for simulating dose reduction. Our method seems an acceptable pragmatic tool for studying the relationship between dose and image quality.**

KEY WORDS: Chest radiographs, digital image processing, digital radiography, dose, noise

INTRODUCTION

Patient dose in chest radiography is relatively low. However, as chest radiography is the most commonly performed X-ray examination, it has significant contribution to the collective dose, and controlling the dose remains an important issue. The obligation for optimization of acquisition techniques for X-ray imaging and limitation of patient dose is formalized in the European Directive.[1]

With the traditional film-screen systems, the range of patient dose in clinical practice was inherently limited by the speed class. Because of the small dynamic range, film-screen radiography images appear underexposed at low dose and overexposed at higher dose.[2] With digital radiography under- or overexposure is not likely to occur because of its wide dynamic range and window functions (window width and window level). The dose level at which optimal image quality is achieved under the condition of "as low as reasonably achievable" should be scientifically established. This could be realized, at least in principle, by performing observer studies in which clinical images acquired at different exposure levels are evaluated. To achieve this, a pure clinical study is preferably avoided because multiple exposures of one and the same patient only for scientific reasons may be considered nonethical.

From the Department of Radiology, C2S, Leiden University Medical Center, Albinusreef 2, 2333 ZA Leiden, The Netherlands.

Correspondence to: Wouter J.H. Veldkamp, Department of Radiology, C2S, Leiden University Medical Center, P.O. Box 9600 2300 RC Leiden, The Netherlands; tel: +31-71-5263689; fax: +31-71-5248256; e-mail: w.j.h.veldkamp@lumc.nl

Online publication 8 February 2009
doi: 10.1007/s10278-008-9104-5

An alternative is simulation of the effect of dose reduction on image quality. A number of researchers reported on methods for simulating reduced-dose images. Such techniques have been applied in digital radiography[3–5] and computed tomography.[6–9] For digital radiography, an accurate simulation method has been described that involves determination (or knowledge) of noise power spectra (NPS) at original and simulated dose levels and the detector quantum efficiency (DQE) to create an image containing filtered noise that is added to the original image to obtain a simulated reduced dose image.[4] In computed tomography (CT), generally, a more simplified model is used for simulating reduced dose, that includes using the pixel standard deviation as a measure of noise, that is used to add white Gaussian noise with certain standard deviation to the original image to obtain a simulated reduced dose image.[6–8] It is unknown to what extent such a simplified model may be applied in conventional (digital) radiography as well. A simplified model would be advantageous, as it could stimulate radiology departments equipped with digital radiography systems to perform dose optimization studies. The purpose of our study was to develop and validate a pragmatic technique for simulating reduced-dose digital chest images, similar to noise simulation techniques used for CT. Additionally, detection performance of simulated lesions in simulated and in real low-dose images was investigated by performing an observer model study. We used the nonprewhitening with eye filter (NPWE) model observer for this purpose.

MATERIALS AND METHODS

Digital Chest System

A slot-scan charge-coupled-device (CCD) digital chest radiography system was used for imaging (ThoraScan Delft Imaging Systems, Veenendaal, The Netherlands). Recent studies have shown good performance of this system compared to conventional state-of-the-art chest radiography systems and other digital chest radiography systems.[10–13]

The ThoraScan chest system is based on a CCD detector array and uses slot-scan acquisition.[10,11] Scanning is performed by using a fan-shaped X-ray beam in combination with a linear solid-state scanning CCD detector. The detector moves synchronously with the fan-shaped X-ray beam. The detector is an assembly of eight CCD chips implemented side-by-side. The scintillator layer that converts the X-rays into visible light is deposited on the fiber-optic plate and consists of cesium iodide.

Image Acquisition

Imaging was performed on a LucAl phantom[14] and an anthropomorphic chest phantom representing the skull and trunk of a 175-cm tall male weighting 73.5 kg (The Phantom Laboratory, Salem, NY, USA; Fig. 1). Images were acquired at 133 kV. The total filtration used was 3 mm Al and 0.3 mm Cu. The use of a scanning X-ray beam requires relatively high mAs. The focus to image plane distance was 183 cm. The LucAl phantom is constructed from slabs of lucite and aluminum, simulating X-ray transmission through the lung region. A radiograph of the phantom gives a flat image. Transmission characteristics of the mediastinum region were simulated by inserting an extra layer of Perspex in the phantom. To provide a look-up table of noise versus mean pixel value and for validation, images were acquired with 198, 103, and 57 mAs for lung and at 154, 102, and 54 exposures for mediastinum transmission equivalent (LucAl phantom). A special system parameter could be adjusted to obtain different tube charges (i.e., the tube current multiplied by the X-ray exposure time, mAs). The relation between the parameter setting and the tube charge (mAs value), however, was not straightforward, which resulted in different tube charges for lung and mediastinum. In addition, images of the anthropomorphic phantom were acquired at 110, 53, and 31 mAs, respectively. Both post-processed and raw image data were acquired. The resolution of the raw image data is equal to the resolution of post-processed images with respect to the vertical direction but twice as large compared to post-processed images with respect to the horizontal direction (Fig. 2).

Simulation of Reduced-Dose Images

A relatively simple method is used for low-dose simulation in this study. The method comprehends measuring noise as standard deviation and adding white noise to images to obtain the desired standard deviation in the resulting images. This is similar to the methodology that is often described for

Fig 1. The anthropomorphic phantom.

simulating lower-dose images in CT. In chest radiography, such an approach could lead to noise spectra that are different from real lower-dose images.

For simulation of reduced-dose images as compared to the 100% reference dose image, the relation between relative detector dose and raw pixel value and the relation between raw pixel value and noise must be known. Quantum noise is linearly related to the square root of the absorbed dose in the detector, which is related to the energy imparted in the detector. In the simulation model, the raw pixel values (after correction for dark current offset) are proportional to the detector dose. Consequently, the quantum noise is proportional to the square root of the pixel values. However, image noise is not necessarily solely determined by quantum noise, as additional noise sources in the system may play a significant role. Therefore, for low-dose simulation in this study, the overall noise (expressed in this study by the sample standard deviation s of pixel values) was measured for different pixel values, and linear interpolation between these measured data was applied to obtain a look-up table with pixel values and their associated noise levels.

To obtain mean raw pixel values approximately linear with the exposure at the CCD detector, dark current was subtracted from each raw LucAl phantom image. The dark current was determined for each CCD by calculating the mean pixel value in the unexposed areas. An example of these dark current CCD columns is shown in Figure 2 for the anthropomorphic phantom. The average pixel value and associated noise level were determined over the CCDs in the exposed area for each of the mAs settings.

The reduced-dose simulation method was programmed in MatLab (MatLab, The MathWorks Inc., Novi, MI, U.S.A.). Reduced-dose images are simulated by linear down scaling of the raw pixel values of a raw image and by adding a random number to each pixel value derived from a Gaussian distribution with zero mean and a standard deviation depending on the pixel value concerned. This results in noise levels that are representative for images acquired at lower mAs settings. Adding Gaussian noise seems admissible. It appeared from our experiments that the noise distribution approximates a Gaussian shape: for higher raw pixel values, the shape of the Poisson distribution approximates a Gaussian distribution. For lower pixel values, influence of additional noise sources (e.g., electronic noise) may become more important, which approximately results in a Gaussian distribution. Furthermore, it was assumed that the actual noise in the images has random phase. By adding white noise,

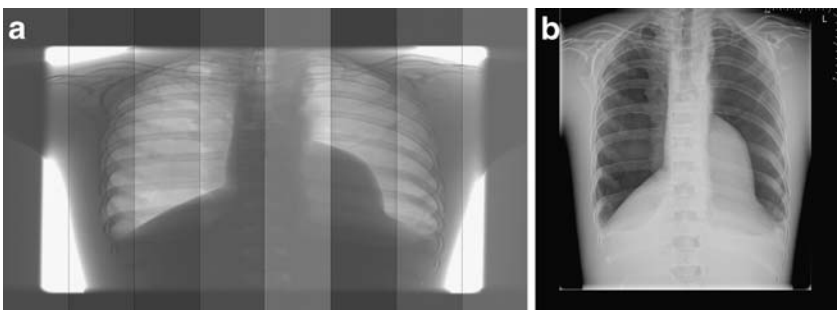

Fig 2. Raw digital radiograph of the anthropomorphic phantom (a) and its corresponding post-processed image (b). Note visualization of the eight CCD columns in the raw image that is caused by the differences in dark current per CCD. Dark current at unexposed areas was measured for each CCD.

noise with random phase is added to the actual image. This is assumed to result in random phase noise.

Once established, the look-up table of pixel values and associated noise can be used to simulate from the raw data any desired dose reduction corresponding to the range of the look-up table. For this purpose, the dose reduction quotient q was defined as the ratio of the desired dose level and the dose level of the original image.

In general, addition of two distributions with respective standard deviations σ_a and σ_b will result in a distribution with a standard deviation σ_c that satisfies:

$$\sigma_c^2 = \sigma_a^2 + \sigma_b^2 \quad (1)$$

Dividing the raw pixel values y with standard deviation σ_y by a dose reduction quotient q will result in new pixel values y/q with standard deviation σ_y/q. In practice, however, reducing the dose of the ThoraScan by a quotient q results in a reduced noise level σ_y/q', with q', a quotient that can be determined from the estimated relation between noise and pixel value in the look-up table. To simulate lower dose images, we added a Gaussian distribution with zero mean and standard deviation σ_G to the downscaled raw image data y/q. Using Eq. 1, it can be shown that σ_G must satisfy the following equation to obtain the desired noise level σ_y/q':

$$\sigma_G^2 = \sigma_y^2 \cdot \frac{q^2 - q'^2}{q^2 \cdot q'^2} \quad (2)$$

After addition of noise, the raw image is post-processed in the standard way.

Validation of Simulating Reduced-Dose Images

Standard Deviation and Mean of Raw Pixel Values

For the LucAl phantom, the 198, 103, and 57 mAs lung images and the 154, 102, and 54 mAs mediastinum images were used to simulate images with reduced mAs values (103, 57, and 22 for the lung and 102, 54, and 25 for the mediastinum configuration, respectively), identical to the real acquisition levels. The simulated images were compared with the real images by evaluation of standard deviation as a measure of noise and mean pixel value.

For the anthropomorphic phantom, the 110 mAs image was used to simulate reduced-dose images at 53 and 31 mAs. These images were compared to the real images acquired with 53 and 31 mAs. Twenty square regions of interest (ROIs) comprising 50× 50 pixels were defined at various locations on the chest phantom images, and mean pixel values and standard deviation values were estimated in these ROIs after dark current subtraction. To minimize the influence of anatomical structures in the measurement of noise, the ROIs were chosen to be relatively small. Care was taken for defining identical locations of the ROIs compared. The locations of the ROIs are shown in Figure 3. The mean difference of mean pixel values and standard deviation values between simulated images and real images was calculated over all 20 ROIs for each comparison.

To gain insight in the variation of standard deviation values between actual images, we compared two real images of the anthropomorphic phantom, both taken with 54 mAs. Twenty ROIs at identical locations in both images were compared.

Noise Power Spectra

In addition to the evaluation of standard deviation and mean of raw pixel values, the NPS of simulated and actual images were calculated and compared. We use these NPS to investigate the accuracy of our method with respect to spatial frequency. For the LucAl phantom, the 103, 57 and 22 mAs lung images were used for this purpose as well as the 102, 54, and 25 mAs mediastinum images. Also a simulated image corresponding to 57 mAs (simulated from 103 mAs) was used for the lung configuration as well as a simulated image corresponding to 54 mAs (simulated from 102 mAs) for the mediastinum

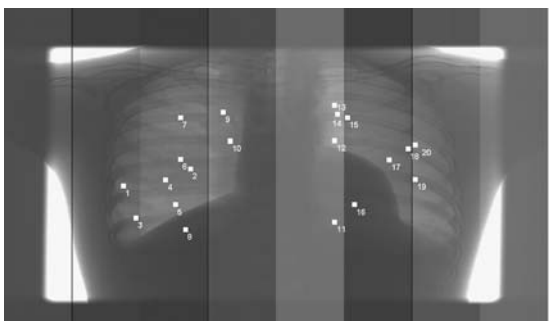

Fig 3. Twenty ROIs were defined of 50×50 pixels (white squares). The locations of the ROIs are depicted by their number in the figure. Noise and mean pixel value were determined in each ROI.

configuration. For calculating an NPS, a method based on the International Electrotechnical Commission standard was used.[15] In short, the procedure was as follows: ROIs containing 256×256 pixels were defined; the ROIs were arranged in overlapping patterns. Two-dimensional Fourier transform was used for calculating the spectra related to the ROIs. An average two-dimensional NPS is obtained by averaging the samples of all the spectra of all ROIs. The NPS was divided by the square of the mean value of the pixels used for analysis. This ratio is referred to as the normalized noise power spectrum and has units of mm^2.

Simulated Lesions

To compare the visibility of low-contrast lesions in simulated and actual images, a method was used to add spherical objects to post-processed LucAl images.[16] For this experiment, mediastinum images were used of 25 and 54 mAs and corresponding simulated images derived from respectively 54 and 102 mAs images. The lesion L was modeled according to:

$$L(k,l) = B \cdot \sqrt{\max\left(R^2 - (k-m)^2 - (l-n)^2, 0\right)}, \quad (3)$$

with (k,l) as a location in the image. This expression creates an object with a radius R and central location (m,n). By altering the brightness B and the radius R, the brightness and size of the lesion could be varied. Blurring of lesions was performed to reduce the appearance of artificial round contours. a number of lesions with different contrast was constructed and added to the post-processed LucAl images. In agreement with an experienced radiologist, the parameters for lesion simulation that gave a realistic appearance were determined and used in the experiments. In the experiments, a circular averaging filter was used with a radius equal to half of the lesion radius R, with R=10 in our experiments. Parameter B was varied (B=15, 30, 45, 60, 75).

Model Observer

The non-prewhitening matched-filter observer with an eye-filter (NPWE) is a mathematical model that has been shown to be similar to human observers for detection tasks in the presence of low-pass noise.[17] Its strategy consists of match filtering the image by the shape of the signal profile filtered by the visual-response function. In our experiments, we considered the signal to be known and always located at the same position (signal known exactly case). The signals used are described in "Simulated Lesions."

In a detection task, the model reaches a decision by comparing test statistics. The test statistics are obtained by cross-correlation between the expected signal and the image.[18] The eye filter used in the model was $E(f)=fe^{-bf}$, with b chosen such that $E(f)$ peaked at 4 cycle per degree. The eye filter is radially symmetric, and f is spatial frequency. In the experiments, a fixed viewing distance of 500 mm from the monitor was assumed.

From the distribution of test statistics, one can compute a discrimination index d'.[18] This index can be used as a measure of detection performance. In this study, d' is used to compare detection performance in simulated and actual low-dose images. The discrimination index can be determined as a function of the square root of lesion signal energy (SE), as is described in.[18]

RESULTS

Simulation of Reduced-Dose Images

The average pixel values and associated noise levels of each of the lung and mediastinum mAs settings for the LucAl phantom images are shown in Table 1. This data was used for constructing the look-up table for simulating images with reduced mAs values.

A near-linear relationship was found between the tube charges and the pixel values for both transmission configurations (Fig. 4), indicating that a linear assumption seems valid for chest radiographs taken at usual clinical exposures. As expected, much lower pixel values were obtained for mediastinum transmissions than for lung transmissions. The noise present in the images appeared not solely quantum limited.

Validation of Simulating Reduced-Dose Images

Table 2 shows the results for the lung configuration of the LucAl phantom. For the source image of 198 mAs, the absolute differences between

Table 1. Noise Versus Mean Pixel Values for LucAl Phantom Images

Lung			Mediastinum		
mAs	Noise (SD)	Mean Pixel Value	mAs	Noise (SD)	Mean Pixel Value
198	14.3	1,093.4	154	3.8	120.8
103	8.2	515.7	102	3.0	75.5
57	5.8	290.3	54	2.3	40.5
22	3.5	112.9	25	1.7	18.6

Images were acquired with four different mAs settings for both lung and mediastinum transmission equivalents.

actual noise measured and simulated noise were <8%, and for raw pixel values, these were <11%. For the source images with 103 and 57 mAs, the absolute differences between actual noise measured and simulated noise were <3%, and for raw pixel values, these were <3%.

Table 3 shows the results for the mediastinum configuration of the LucAl phantom. For all source images, the absolute differences between simulated noise compared to noise in real images were <5%. The absolute differences for simulated raw pixel values were <6% and appear to decrease for lower mAs source images. The relative differences in pixel values and measured noise between real and simulated images of the LucAl phantom seem to be within acceptable limits for dose reduction simulation for both lung and mediastinum transmission equivalents.

Table 4 shows the 20 pixel values and noise values of the various ROI locations in the anthropomorphic phantom image, where a 53 mAs image was simulated from a 110-mAs image, and was compared to the values in an actual 53-mAs image. The mean of the 20 relative differences with respect to simulated noise was 0.2% (standard deviation, 7.2). For the simulated pixel values, the mean of the 20 relative differences was −0.6% (standard deviation, 0.3).

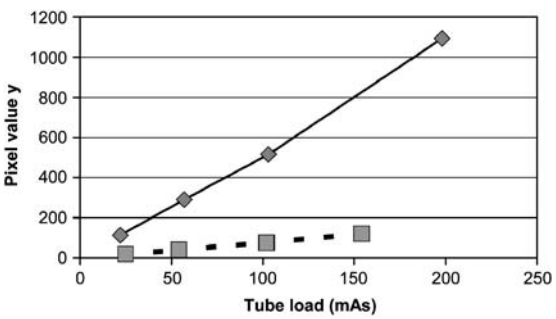

Fig 4. Pixel values for transmission through the LucAl phantom as function of tube charge (mAs). Note the near-linear relationship for the lung configuration (solid line), as well as the mediastinum configuration (dotted line).

For the 31 mAs image simulated from a 110-mAs image, the mean of the 20 ROI differences between simulated and actual noise was 1.9% (standard deviation, 7.1). For the simulated pixel values, the mean difference of the 20 ROIs was 0% (standard deviation, 0.2).

Comparing 20 ROIs of two real 54-mAs anthropomorphic phantom images, differences were found in the range of −11% to 20% (mean=−0.1%, standard deviation=6.5), whereas the differences that are given in Table 4 vary between −11% and 12%. Note that the differences between values found for real and simulated 53 mAs images are comparable to differences found between two real 54 mAs images. This implies that the relative difference in pixel values and measured noise between real and simulated images of the anthropomorphic phantom seem to be within acceptable limits for dose reduction simulation.

Noise Power Spectra

The normalized NPS are represented in Figure 5. The NPS of the simulated images were at the same level as the NPS of the actual dose images, although the NPSs did not precisely fit. The accuracy of the simulation method showed best results at low frequencies (approximately 1–3 cycles per millimeter) but decreased with lower and higher spatial frequencies.

Simulated Lesions

An example of the appearance of a simulated low-contrast lesion in simulated and actual lower dose images is shown in Figure 6. Although the visual appearance between the actual and simulated dose images is quite similar, slight differences

Table 2. LucAI Phantom Images in Lung Configuration

mAs	Real Image Noise	Simulated Image Noise	Difference (%)	Real Image Pixel Value	Simulated Iamge Pixel Value	Difference (%)
Source image, 198 mAs						
103	8.2	8.8	7.3	515.7	569.3	10.4
57	5.8	6.0	3.4	290.3	315.8	8.8
22	3.5	3.7	5.7	112.9	122.9	8.9
Source image, 103 mAs						
57	(5.8)	5.7	−1.7	(290.3)	285.4	−1.7
22	(3.5)	3.4	−2.9	(112.9)	110.5	−2.1
Source image, 57 mAs						
22	(3.5)	3.5	0.0	(112.9)	112.0	−0.8

Dose reduction from 198, 103, and 57 mAs source images in lung configuration. Numbers between brackets represent the same measurements as the rows above.

in visual appearance may be observed in zoomed details.

Model Observer

Also, the detectability of simulated lesions was investigated using the NPWE model observer. The model observer showed good agreement in lesion detection performance in simulated and actual images with slightly worse detectability for simulated lower-dose images. This is shown in Figure 7 by the discrimination index d' versus the square root of signal energy SE in simulated lesions (B= 15, 30, 45, 60, and 75 for simulating lesions).

CONCLUSIONS AND DISCUSSION

A technique is presented for simulating reduced dose images. The method gives promising results and may be used in clinical studies to evaluate detectability and discrimination of lesions in digital chest images under different dose levels without the need for taking extra radiographs. The technique was validated for chest imaging, where the lung and mediastinum transmission profiles were separately analyzed. Although the study was performed on a digital radiography system with charge-coupled device technology, the reduced-dose simulation method is potentially applicable to any digital radiography system.

In clinical practice, radiation doses used for imaging vary substantially among technically different digital chest systems. Moreover, studies using contrast-detail phantoms and simulated chest lesions have shown that the image quality, as well as the detection of lesions, varies between different systems, where the technical system designs rather than the dose settings are seem responsible for system performance.[13,19] Because of the large variety of digital chest systems available on the market, it seems a challenge to define optimal dose- and post-processing settings for individual digital radiography systems. Our proposed method may facilitate investigating image quality as a function of radiation dose, as it is relatively easy to apply.

Table 3. LucAI Phantom Images in Mediastinum Configuration

mAs	Real Image Noise	Simulated Image Noise	Difference (%)	Real Image Pixel Value	Simulated Image Pixel Value	Difference (%)
Source image, 154 mAs						
102	3.0	3.1	3.3	75.5	79.7	5.6
54	2.3	2.3	0.0	40.5	42.3	4.4
25	1.7	1.7	0.0	18.6	19.7	5.9
Source image, 102 mAs						
54	(2.3)	2.2	4.3	(40.5)	39.7	−2.0
25	(1.7)	1.7	0.0	(18.6)	18.3	−1.6
Source image, 54 mAs						
25	(1.7)	1.7	0.0	(18.6)	18.4	−1.1

Dose reduction from 154, 102, and 54 mAs source images in mediastinum configuration. Numbers between brackets represent the same measurements as the rows above.

Table 4. ROI Evaluation on the Anthropomorphic Phantom

	ROI Number	Real Noise	Simulated Noise	Relative Difference (%)	Real Pixel Value	Simulated Pixel Value	Relative Difference (%)
	1	4.4	4.9	11.4	402.5	399.0	−0.9
	2	5.3	5.3	0.0	362.9	359.9	−0.8
	3	17.8	19.6	10.1	405.5	406.6	0.3
	4	5.8	5.2	−10.3	447.4	443.3	−0.9
	5	6.4	6.1	−4.7	496.3	491.6	−0.9
	6	18.1	17.8	−1.7	439.9	439.3	−0.1
	7	7.3	6.6	−9.6	453.9	450.4	−0.8
	8	3.1	3.3	6.5	273.0	272.0	−0.4
	9	5.1	5.1	0.0	469.6	465.1	−1.0
	10	5.9	5.5	−6.8	442.6	440.2	−0.6
	11	3.2	3.2	0.0	464.1	462.9	−0.3
	12	7.1	6.6	−7.0	622.7	620.2	−0.4
	13	6.6	7.1	7.6	624.0	620.6	−0.5
	14	8.8	9.3	5.7	607.9	604.7	−0.5
	15	6.4	5.8	−9.4	426.4	423.3	−0.7
	16	2.7	2.7	0.0	292.4	290.5	−0.6
	17	5.3	4.9	−7.5	441.4	438.6	−0.6
	18	11.7	12.0	2.6	389.5	387.5	−0.5
	19	4.1	4.3	4.9	459.0	457.3	−0.4
	20	4.2	4.7	11.9	491.1	487.4	−0.8
Mean				0.2			−0.6
Standard deviation				7.2			0.3

Pixel values and noise were measured in 20 ROIs of a 53 mAs image that was simulated from a 110-mAs image. These values were compared with a real 53-mAs image.

A well-established method for reduced-dose simulation that has been previously described uses detective quantum efficiency (DQE) and NPS at the original and simulated dose levels to create an image containing filtered noise.[4] The method provides for simulated images containing noise that, in terms of frequency content, agree well with original images at the same dose levels. However, this ideal dose reduction simulation method requires specialized equipment to measure DQE and NPS, which is not available in most clinical practices. Conversely, the simplified method for simulating reduced dose images proposed in our study does not involve determination or knowledge of NPS and DQE, and may be applied in any radiology department for investigating the relation between dose and image quality.

A systematic difference in NPS was found between the lung and mediastinum configuration. This can be explained by the NPS that were divided by the square of the mean value of the pixels used for analysis. The ratio refers to noise normalized by the mean signal at the detector. Because of the higher signal to noise ratio for the lung configuration compared to the mediastinum configuration, the normalized noise is lower in the lung than in the mediastinum configuration.

The NPS for both mediastinum and lung configuration showed higher noise power for higher frequencies and lower noise power for lower frequencies, although on average, the NPS levels were comparable. By adding white noise to the existing noise, the resulting noise will be "more white." As a consequence of the technique used, the standard deviations in simulated and actual low-dose images is comparable where the standard deviation is related to the average noise power. This means that the high-frequency noise will be higher compared to the actual low-dose images, whereas the low-frequency noise will be lower compared to the actual low-dose images, depending on the amount of noise that is added. The simulation method showed better fit at lower frequencies (approximately 0–2.5 cycles per millimeter) than at higher frequencies (approximately >2.5 cycles per millimeter). It should be noted that the actual overall noise power is dominated by the lower frequency noise, as noise power decreases substantially with increasing spatial frequency. Furthermore, in the post-processed images, the resolution in

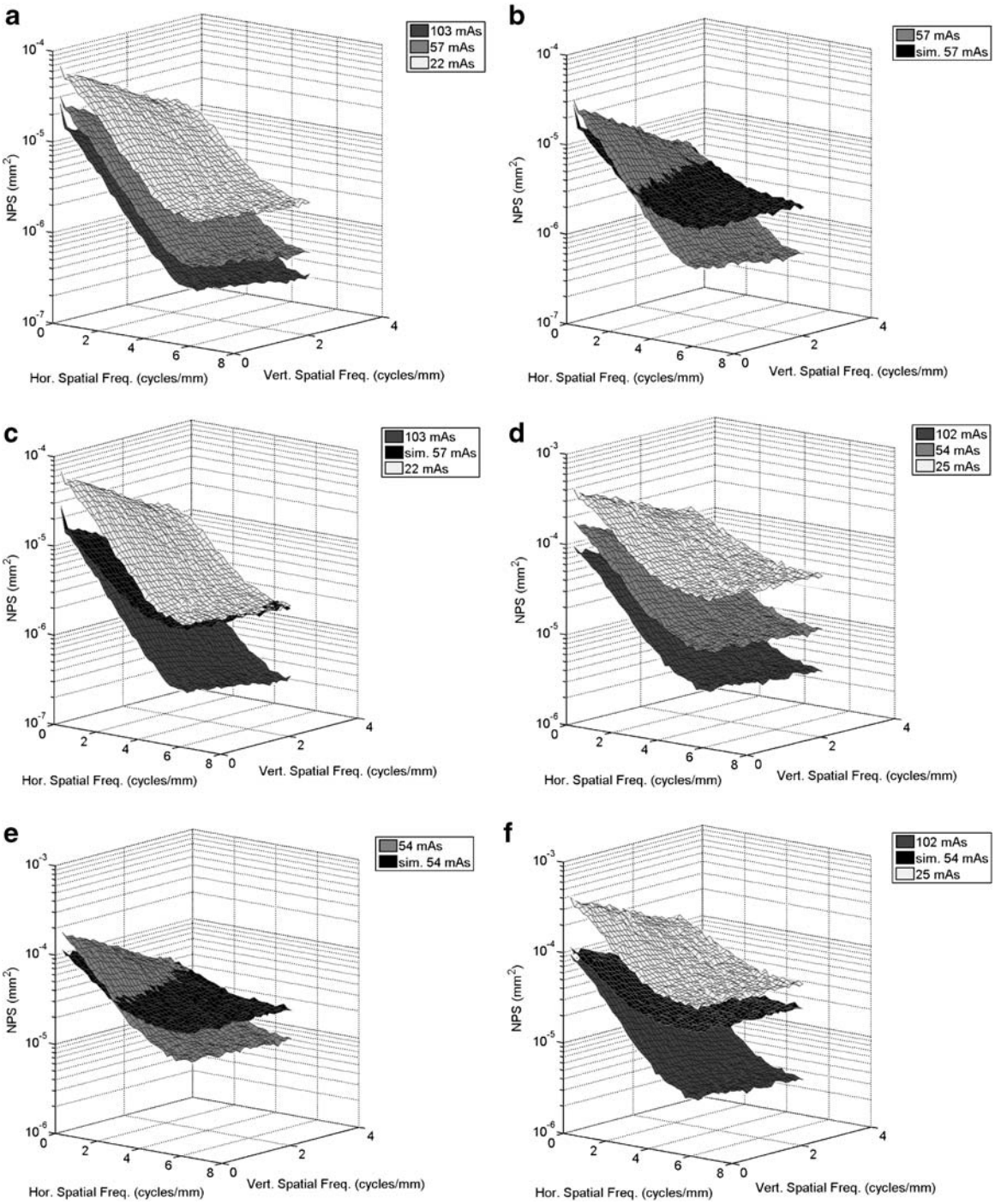

Fig 5. Normalized NPS for the lung configuration (a–c) and mediastinum configuration (d–f). NPS for actual images (a, d). NPS for an actual dose and corresponding simulated dose image (b, e). NPS for a simulated reduced dose image as compared to the actual dose images (c, f). Note the clear difference in NPS between the actual mAs value images (a, d). The NPS of the simulated reduced-dose images are at the same level as their corresponding actual dose images (b, e), although these NPS do not precisely fit as the simulated images show slightly higher noise levels for higher spatial frequencies and slightly lower noise levels for lower spatial frequencies. Note that this effect is more pronounced for the lung configuration than for the mediastinum configuration.

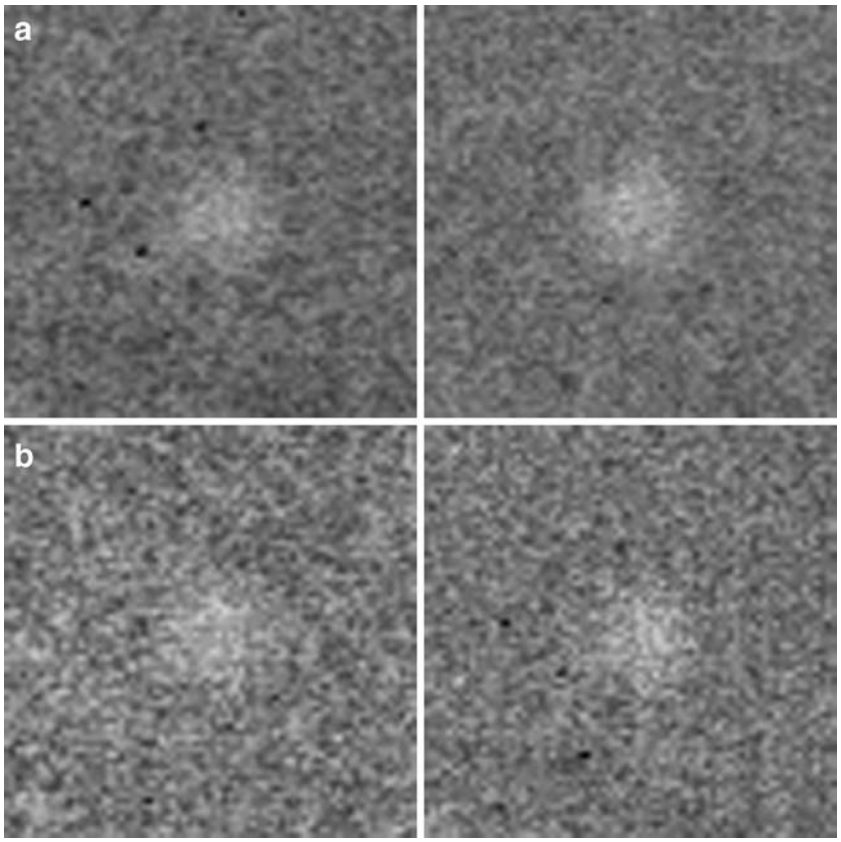

Fig 6. Zoomed detail of a 0.162 mm pixel size matrix showing simulated low contrast nodular lesions (parameter B = 15) in mediastinum parts of the anthropomorphic phantom. Details of actual images are shown at the left, whereas details of simulated images are shown at the right. The images correspond to 54 mAs (a) and 25 mAs (b). Visually, the actual and simulated 54-mAs images appear quite similar (a). At 25 mAs, the simulated image seems to have a more uniform noise pattern than the actual image, although mean pixel variation and variance was in fact equal in both images (b).

the horizontal direction is decreased to halve the resolution of the raw images in horizontal direction (approximately 3.1 cycles per millimeter). This means that a substantial part of the deviation between simulated and actual images has been calculated for raw-image data but is not relevant for post-processed images used for diagnostic evaluation.

Visual inspection showed quite similar appearance of zoomed simulated reduced dose images as compared to the actual dose images. The appearance of noise and low-contrast objects appeared visually comparable for a human observer, and in our opinion, the presented simplified model seems sufficient for investigating trends in diagnostic accuracy as a function of dose reduction. This was confirmed by the NPWE model observer experiment. The model observer showed slightly worse detectability for simulated lower dose images. The difference in discrimination index d' between actual and simulated images increased for lower dose levels.

Some technical issues should be taken in consideration. As observed for the LucAl phantom, the noise in the images was not solely quantum

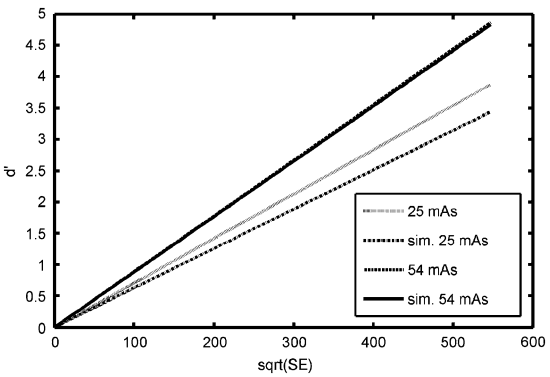

Fig 7. NPWE model observer performance with respect to simulated lesions in actual and simulated lower-dose images. Discrimination index d′ is a measure of detection performance and given as a function of the square root of signal energy SE in simulated lesions (B = 15, 30, 45, 60, 75).

limited, as the variance (squared standard deviation) of the actual pixel data did not precisely fit a linear function. This can be explained by additional noise sources that play a role in the imaging chain. Because of these observed additional noise sources, we did not use the square root relation between noise and raw pixel values but instead used the measured data from Table 1 to construct a look-up table to provide more precise noise values to add for simulating reduced-dose images. Although the amount of noise caused by the system itself is relatively limited in terms of contributing as noise source in final images,[20] use of look-up tables for simulated reduced-dose images with the method described is advisable for optimal representation of actual doses and because the amount of additional noise sources may vary between different system technologies.

For the lung source images with the highest (198) mAs values, the difference found in noise and raw pixel values between simulated and real images were larger (maximum, 7.3% and 10.4%, respectively) than for source images acquired at lower mAs values. This can be attributed to the non-linearity of raw pixel values as a function of mAs in this range of higher mAs values where our model assumes a linear relation. It should be noted that image acquisition of the LucAl phantom with the ThoraScan under clinical conditions, including automatic exposure control, corresponds with 82 mAs.[10] This implies that the method would be used for considerably lower mAs settings than 198 mAs when applied to clinical chest radiographs as source images.

Study Limitation

The "simplified" method evaluated for digital chest radiography in our study is a known and accepted method for simulating reduced-dose images in computed tomography (CT).[7–9] Radiographic image noise varies with spatial frequency, where variation of noise power with spatial frequency is of less importance in raw CT data than in raw digital radiography images. First, frequency dependency of noise power in reconstructed CT images is mainly the result of the filtered back projection. The frequency dependency of noise power in raw CT data is, therefore, of less importance. Moreover, in raw CT data, the frequency dependency is limited because linear CT detectors contain septa between their detector elements. These septa prevent spreading of light to other detector elements, hereby preserving the high frequency content of the noise power in raw CT data. Such septa are not present in X-ray detectors used in digital radiography. A study limitation of our method could be that the variation of noise power with spatial frequency is not modeled. The unknown relation between spatial frequency and noise may affect the visual appearance and detectability.

In conclusion, we have validated a method for simulating reduced-dose images in digital chest radiography that does not include measurements of DQE or NPS and can be potentially applied to any digital radiography system in any radiology practice. The proposed method can be considered a reasonable option for investigating trends regarding diagnostic image quality as a function of dose reduction.

ACKNOWLEDGMENT

Henk Venema, PhD (Academic Medical Center, Amsterdam), is gratefully acknowledged for providing valuable recommendations.

REFERENCES

1. European Commission. Council Directive 97/43/EURATOM of 30 June 1997 on health protection of individuals against the dangers of ionising radiation in relation to medical exposure, and repealing. Directive 84/466/ EURATOM. Official Journal of the European Communities L-180/22, 9 July 1997

2. Chotas HG, Dobbins JT, III, Ravin CE: Principles of digital radiography with large-area electronically readable detectors: a review of the basics. Radiology 210:595–599, 1999

3. Treiber O, Wanninger F, Fuhr H, Panzer W, Regulla D, Winkler G: An adaptive algorithm for the detection of microcalcifications in simulated low-dose mammography. Phys Med Biol 48:449–466, 2003

4. Bath M, Hakansson M, Tingberg A, Mansson LG: Method of simulating dose reduction for digital radiographic systems. Radiat Prot Dosimetry 114:253–259, 2005

5. Saunders RS, Jr, Samei E: A method for modifying the image quality parameters of digital radiographic images. Med Phys 30:3006–3017, 2003

6. van Gelder RE, Venema HW, Florie J, Nio CY, Serlie IW, Schutter MP, van Rijn JC, Vos FM, Glas AS, Bossuyt PM, Bartelsman JF, Lameris JS, Stoker J: CT colonography: feasibility of substantial dose reduction—comparison of medium to very low doses in identical patients. Radiology 232:611–620, 2004

7. van Gelder RE, Venema HW, Serlie IW, et al: CT colonography at different radiation dose levels: feasibility of dose reduction. Radiology 224:25–33, 2002

8. Frush DP, Slack CC, Hollingsworth CL, Bisset GS, Donnelly LF, Hsieh J, Lavin-Wensell T, Mayo JR: Computer-

simulated radiation dose reduction for abdominal multidetector CT of pediatric patients. AJR Am J Roentgenol 179:1107–1113, 2002

9. Mayo JR, Whittall KP, Leung AN, et al: Simulated dose reduction in conventional chest CT: validation study. Radiology 202:453–457, 1997

10. Veldkamp WJ, Kroft LJ, Mertens BJ, Geleijns J: Comparison of image quality between a digital slot-scan CCD chest radiography system and AMBER and Bucky screen-film radiography chest systems. Radiology 235:857–866, 2005

11. Samei E, Saunders RS, Lo JY, Dobbins JT, 3rd, Jesneck JL, Floyd CE, Ravin CE: Fundamental imaging characteristics of a slot-scan digital chest radiographic system. Med Phys 31:2687–1298, 2004

12. Kroft LJ, Geleijns J, Mertens BJ, Veldkamp WJ, Zonderland HM, de Roos A: Digital slot-scan charged coupled device chest radiography versus AMBER and Bucky screen-film radiography: detection of simulated chest nodules and interstitial disease using a chest phantom. Radiology 231:156–163, 2004

13. Kroft LJ, Veldkamp WJ, Mertens BJ, Boot MV, Geleijns J: Comparison of eight digital chest radiography systems: variation in detection of simulated chest disease. AJR 185:339–346, 2005

14. Conway BJ, Butler PF, Duff JE, et al: Beam quality independent attenuation phantom for estimating patient exposure from x-ray automatic exposure controlled chest examinations. Med Phys 11:827–832, 1984

15. International Electrotechnical Commission: Medical electrical equipment—characteristics of digital X-ray imaging devices—part 1: determination of the detective quantum efficiency, Geneva, Switzerland: International Electrotechnical Commission, 2003

16. te Brake GM, Karssemeijer N: Single and multiscale detection of masses in digital mammograms. IEEE Trans Med Imaging 18:628–639, 1999

17. Bochud FO, Valley JF, Verdun FR, Hessler C, Schnyder P: Estimation of the noisy component of anatomical backgrounds. Med Phys 26:1365–1370, 1999

18. Reiser I, Nishikawa RM: Identification of simulated microcalcifications in white noise and mammographic backgrounds. Med Phys 33:2905–2911, 2006

19. Veldkamp WJ, Kroft LJ, Boot MV, Mertens BJ, Geleijns J: Contrast-detail evaluation and dose assessment of eight digital chest radiography systems in clinical practice. Eur Radiol 16:333–341, 2006

20. Håkansson M, Båth M, Börjesson S, Kheddache S, Grahn A, Ruschin M, Tingberg A, Mattsson S, Månsson LG: Nodule detection in digital chest radiography: summary of the radius chest trial. Radiat Prot Dosim 114:114–120, 2005